

# A high-resolution view of the jets in 3C465

E. Bempong-Manful<sup>1,2</sup>, M.J. Hardcastle<sup>1</sup>, M. Birkinshaw<sup>2</sup> and the e-MERLIN Jets Legacy Project

<sup>1</sup>School of Physics, Astronomy and Mathematics, University of Hertfordshire

<sup>2</sup>School of Physics, University of Bristol

## Introduction

Relativistic plasma ejected from SMBHs at the centres of galaxies is known to play a key role in the AGN feedback cycle, and consequently the formation and evolution of structure in the universe. However, the physics driving the observed jet structure in these cosmic outflows including where and how particles are accelerated in the jets and hotspots, among other questions, remains open. As part of a project that aims to resolve some of these key questions in extragalactic jet physics, we present new high-resolution and high-sensitivity studies on the nature of jets in the powerful FR I WAT source 3C465, using the first ever deep transverse resolved radio observations from e-MERLIN, and with complementary observations from the VLA.

## Data and Methods

### Summary of Observations

Band (GHz)	VLA observations				e-MERLIN observations			
	A configuration	B configuration	Epoch-1		Epoch-2			
	Date	Time (h)	Date	Time (h)	Date	Time (h)	Date	Time (h)
1	Oct 31	1.2	May 28	1.2	Apr 12	19	Apr 13	19.3
(-1.5)	2012		2012		2015		2015	

**Data calibration & imaging:** The data were calibrated and imaged using the standard procedure in CASA and AIPS respectively for the VLA and e-MERLIN datasets. As a standard technique in all VLBI observations, we performed fringe-fitting on the e-MERLIN datasets prior to calibration.

**Data combination & mapping:** The combination was executed in the Fourier plane to allow for better constraints on the CLEAN algorithm (see Biggs & Ivison, 2008) following down-weighting of the VLA data.

**Resolution matching:** For accurate determination of the spectral index,  $\alpha$ , we convolved our 1.5 GHz map, and the 8.5 GHz map (obtained from Hardcastle & Sakelliou, 2004) to equivalent resolutions to allow for consistent flux recovery.

## Radio Maps

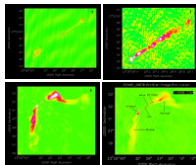


**Figure 1:**  
**Top:** Left:  $0.27 \times 0.15''$  e-MERLIN map. Right: inner 5 kpc radius showing the bright knots at the jet base.  
**Bottom:**  
 Left:  $1.4 \times 1.1''$  VLA (A+B configuration) map. Right:  $0.39 \times 0.37''$  combined e-MERLIN plus VLA map.

## Conclusion and Future Work

The jet and hotspots have a lower than the material (plumes) into which they flow as expected from the standard model. For future work, we aim to observe over a broad range of frequencies to study in detail the deviations from power law spectra and as well, investigate the orientation and degree of ordering of magnetic field in the jet base.

## Results and Discussion

### Spectral index map:



**Figure 2:** Map of  $\alpha$ , constructed from maps made at two frequencies ( $\sim 1.5$  and  $\sim 8.5$  GHz) at  $1.5''$  resolution. With the exception of the unresolved core, which is partially optically thick with  $\alpha \sim -0.4$ , the emission typically has  $-0.5 \leq \alpha \leq -0.8$  over the jet region and  $-1.1 \leq \alpha \leq -2.3$  in the plumes, and is plotted at  $3\sigma$  rms noise cut-off in total intensity.

**Jets, knots, hotspots & plumes:** The NW jet is well resolved and has a cross-sectional width of  $\sim 0.32$  arcsec and termination length of  $\sim 29.8$  kpc. At e-MERLIN resolution (see Fig. 1) we infer multiple bright knots at the NW jet base. Variations in jet-environment interactions at the hotspot regions account for the apparent asymmetry in the physical size and shape of the two components, whereas 2-D projection effects plausibly account for the observed asymmetry in physical size and structure of the two large scale components (plumes).

**Jet speed & sidedness ratio:** Following the procedure defined by Hardcastle et al. (1998), we obtain a sidedness ratio of 15; and by defining the jet/counterjet flux densities ratio as;

$$J = \left( \frac{1 + \beta_j \cos \theta}{1 - \beta_j \cos \theta} \right)^{\delta}$$

we obtain lower limit values of  $0.5c$  and  $61^\circ$  respectively for the jet speed,  $\beta_j$ , and angle to the line of sight,  $\theta_j$ .

### Spectral profiles:

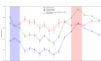
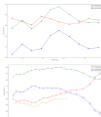


**Figure 3:** Top:  $\alpha$  along the NW jet axis versus distance from the core.  $\langle \alpha_{NW} \rangle = -0.7$ . Flattening of  $\alpha$  within the first 4.45 kpc in the jet provides evidence of ongoing particle acceleration at the jet base, consistent with observations from X-ray studies (see Hardcastle et al. 2006).



**Middle:** Distribution of  $\alpha$  for the two hotspots.

**Bottom:** Distribution of  $\alpha$  for the two plumes.

**Constraints on particle acceleration:** The first-order Fermi process at mildly relativistic shocks is the most probable acceleration mechanism at play in 3C465, and, consistent with earlier work by Laing et al. (2013), we infer two acceleration mechanisms; (a) when bulk flow speeds,  $\beta_j \geq 0.5$ , and (b) when flow speeds,  $\beta_j$  is less than  $\sim 0.5$ . The first case can accelerate electrons to high Lorentz factors, whereas the second must occur at slower speeds and larger distances.

## References

- Biggs & Ivison (2008). *MNRAS*, 385, 893–904.  
 Hardcastle & Sakelliou (2004). *MNRAS*, 349, 560–575.  
 Hardcastle et al. (2006). *MNRAS*, 359, 1007.  
 Laing et al. (2013). *MNRAS* 432, 1114–1132.